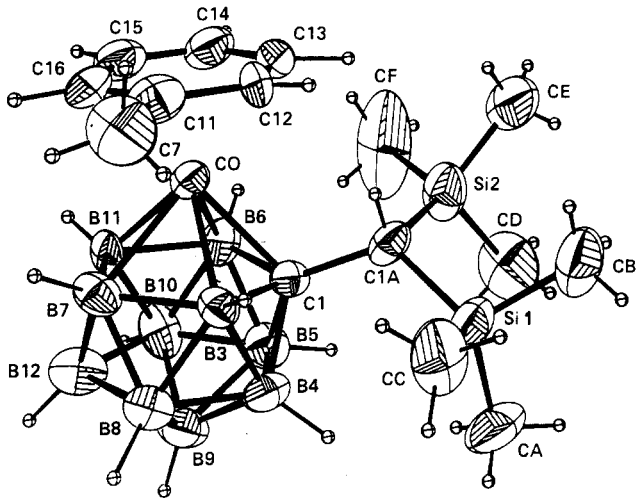

Figure 5. ORTEP drawing of the molecular structure of 2-(η^6-$C_6H_5CH_3$)-1-[$((CH_3)_3Si)_2CH$]-2,1-$CoCB_{10}H_{10}$ (VI). Non-hydrogen atoms are shown as 50% thermal ellipsoids. The hydrogen atoms have been arbitrarily assigned artifically small thermal parameters.

As was observed in V, the planes of the two ligands are tilted with respect to each other (7.6°) in order to minimize the repulsions between the bis(trimethylsilyl)methyl group and the η^6-toluene unit. The average of the cobalt to ring-carbon distances (2.14 Å) is the same as that observed in, for example, (η^6-$C_6H_5CH_3$)$Co(C_6F_5)_2$;[19] however, the carbons near the bis(trimethylsilyl)methyl group have longer Co–C distances, C12–Co = 2.17 (1) Å and C13–Co = 2.15 (1) Å, than those on the opposite side of the toluene ring, C16–Co = 2.10 (1) Å and C15–Co = 2.117 (1) Å.

In general, the carborane interatomic distances are again found to be within the normal ranges and are similar to those in V; however, the distances between the atoms on the bonding face of the carborane (C1, B3, B7, B11 and B6) are somewhat shortened compared to the analogous distances in V.

In summary, the results reported herein have demonstrated that the carborane 9-$(CH_3)_2$S-7-[$(((CH_3)_3Si)_2CH$]-$CB_{10}H_{11}$ can function as a versatile ligand by coordinating to transition metals as either the [$((CH_3)_3Si)_2CH]CB_{10}H_{10}^{3-}$ or $(CH_3)_2S$–[$(((CH_3)_3Si)_2CH]CB_{10}H_9^{2-}$ anions. Steric interactions between the other ligands on the metal and the cage-bound bis(trimethylsilyl)methyl group, however, can lead to significant geometric distortions. We are presently investigating the development of new synthetic routes to the parent carborane *nido*-$(CH_3)_2S$–$CB_{10}H_{12}$ so that the chemistry of this potentially useful ligand can be more fully explored.

Acknowledgment. We thank the Army Research Office and the National Science Foundation for the support of this research.

Registry No. I, 110717-83-4; II, 110743-51-6; III, 110717-84-5; IV, 110717-85-6; V, 110743-52-7; VI, 110743-53-8; PPh_3, 603-35-0; 9-$(CH_3)_2$S-7-[$((CH_3)_3Si)_2CH]CB_{10}H_{11}$, 105335-10-2; ($\eta$-$C_5H_5$)$Co(CO)_2$, 12078-25-0; [($\eta$-$C_5H_5$)$Ni(CO)]_2$, 12170-92-2; Na[2-(($(C-H_3)_3Si)_2CH)CB_{10}H_{10}]^-$, 105309-51-1.

Supplementary Material Available: Tables of general temperature factors, intermolecular angles, molecular planes, and hydrogen positions for I, V and VII (29 pages); listings of observed and calculated structure factors for I, V, and VI (28 pages). Ordering information on any current masthead page.

(19) Radonovich, L. J.; Klabunde, K. J.; Behrens, C. B.; McCollor, D. P.; Anderson, B. B. *Inorg. Chem.* **1980**, *19*, 1221–6.

Alkyl and η^2-Acyl Complexes of Iron(II)

Giuseppe Cardaci,* Gianfranco Bellachioma, and Pierfrancesco Zanazzi

Dipartimento di Chimica and Dipartimento di Scienze della Terra, sez. Cristallografia, Università di Perugia, I-06100 Perugia, Italy

Received May 18, 1987

The reduction with sodium amalgam in acetonitrile (MeCN) of $[Fe(CO)_2L_2X_2]$ (X = Cl, Br, I; L = PMe_3, PMe_2Ph, $P(n\text{-}Bu)_3$, $PMePh_2$, $P(i\text{-}Bu)_3$, $P(i\text{-}Pr)_3$, $PEtPh_2$, PPh_3) gives a mixture of two different complexes in equilibrium. One is probably the cluster complex $[Fe(CO)_2L_2]_3$, isoelectronic with $[Fe_3(CO)_{12}]$; the other is the complex $[Fe(CO)_2L_2(MeCN)]$. The mixture in equilibrium reacts with RI (R = CH_3, C_2H_5) to give oxidative addition products. With L = PMe_3, PMe_2Ph, and $P(n\text{-}Bu)_3$ the products are the alkyl complexes $[Fe(CO)_2L_2(R)I]$. With L = $PMePh_2$, $PEtPh_2$, $P(i\text{-}Bu)_3$, and PPh_3 the reaction products are the η^2-acyl complexes $[Fe(CO)L_2(\eta^2\text{-}COR)I]$. Complex $[Fe(CO)(PMePh_2)_2(\eta^2\text{-}COCH_3)I{\cdot}2CH_2Cl_2]$ was analyzed by the single-crystal X-ray diffraction method. It crystallizes in the monoclinic space group $P2_1/n$ with lattice parameters a = 23.603 (4) Å, b = 12.256 (3) Å, c = 12.318 (3) Å, and β = 97.08 (2)°; it contains four molecules per cell. The structure was solved by using 2642 observed reflections and refined to R_w = 0.062. The electronic and steric features of the phosphine ligands, which stabilize the η^2-acyl structure, are discussed, the steric hindrance appearing to be the most important factor for the same metal. The effect of the nature of the metal is also discussed, the stability of the η^2-acyl structure being correlated with the number of the d electrons on the metal in its formal oxidation state.

Introduction

The study of the synthesis and characterization of alkyl complexes of transition metals is valuable, since their reactivity with carbon monoxide can yield information about the mechanism and stereochemistry of the insertion of this ligand in the metal–alkyl bond.[1] Much information on the stereochemistry of the insertion of carbon monoxide has been obtained in the study of the octahedral complexes of Mn.[2] The alkyl cyclopentadienyl complexes of iron(II) have also been extensively studied,[3] but, due to their

(1) (a) Calderazzo, F. *Angew. Chem., Int. Engl. Ed.* **1977**, *16*, 299–311. (b) Wojcicki, A. *Adv. Organomet. Chem.* **1973**, *11*, 87–145.

(2) (a) Noack, K.; Calderazzo, F. *J. Organomet. Chem.* **1967**, *10*, 101–104. (b) Flood, T. C.; Jansen, T. E.; Statler, J. A. *J. Am. Chem. Soc.* **1981**, *103*, 4410–4414.

(3) Attig, T. G.; Wojcicki, A. *J. Organomet. Chem.* **1974**, *82*, 397–415.

0276-7333/88/2307-0172$01.50/0

relatively low symmetry, it is difficult to obtain information about the stereochemistry at the metal. On the other hand, these complexes have proved very useful for clarifying the stereochemistry at the alkyl carbon in the insertion reaction.[4]

Taking this into account, octahedral alkyl complexes of iron(II) should be of great interest. However only a few of these complexes have been described in the literature, viz., $[Fe(CO)_2(PMe_3)_2(CH_3)I]$,[5] $[Fe(CO)_3(PMe_3)_2(CH_3)]BPh_4$,[6] and $[Fe(CO)_3(Diars)(CH_3)]BF_4$.[7] These complexes were obtained via the oxidative addition of CH_3I to the disubstituted derivatives $[Fe(CO)_3(PMe_3)_2]$ and $[Fe(CO)_3(Diars)]$. Owing to the steric hindrance, this reaction cannot be extended to other phosphine ligands or alkyl halides. However, various η^2-acyl complexes with different metals are described and characterized in the literature,[8] but up to now, there has been no systematic approach for studying the electronic and steric features that stabilize these structures. Bearing this in mind, it is essential to find a preparative method for the alkyl complexes which allows us to vary the ligands and the alkyl groups. A convenient method for preparing the alkyl complexes of iron(II) is the formation in situ of the unsaturated intermediate $[Fe(CO)_2L_2]$, which should undergo oxidative addition. The formation of $[Fe(CO)_2L_2]$ has been hypothesized in many processes (substitution,[9] reduction,[10] etc.), but it is very reactive and quickly gives $[Fe(CO)_4L]$ and $[Fe(CO)_3L_2]$ before reacting with alkyl halides.

We have recently found that the $[Fe(CO)_2L_2]$ intermediate can be stabilized by a labile ligand[11] such as acetonitrile; this allows us to obtain an oxidative addition with alkyl halides. In this paper we show the results obtained by using this reaction method.

Experimental Section

Acetonitrile (MeCN) was purified as described in the literature;[12] diethyl ether, *n*-hexane, and benzene were purified by refluxing with Na and distilled under nitrogen; tetrahydrofuran (THF) was reacted with Na and benzophenone and distilled immediately before use; dichloromethane was distilled from P_2O_5; I_2, Br_2, Cl_2, and $Fe(CO)_5$ were commercial products; trimethylphosphine was prepared following the method described by Schmidbaur;[13] all the other phosphine ligands were commercial products (Strem) and were used without further purification. $[Fe(CO)_4Br_2]$ was prepared following the method described by Basolo et al.;[14] $[Fe(CO)_4Cl_2]$ was prepared following the method of Hieber et al.[15]

All the reactions were carried out under nitrogen. The infrared spectra were recorded on a Perkin-Elmer 983 spectrophotometer. The ^1H NMR spectra were recorded with a JEOL CHL-60 spectrophotometer or with a Varian EM 390 spectrometer, using tetramethylsilane (TMS) as the internal reference. The elemental analyses were carried out with a Carlo Erba 1106 elemental analyzer.

Preparation of the Complexes. $[Fe(CO)_2(PMe_2)_2Br_2]$ (1). (a) Method I. Equimolar quantities of $[Fe(CO)_3(PMe_3)_2]$[5] (3.5 g) and Br_2 (2.0 g) were mixed in THF (400 mL). The formation of a solid was immediately observed. It corresponds to the ionic complex $[Fe(CO)_3(PMe_3)_2Br]Br$ (ν_{CO} 2116, 2061, and 2047 cm^{-1} in CH_2Cl_2). When the suspension is stirred under nitrogen at the boiling point, the formation of 1 was complete in three hours (ν_{CO} 2025 and 1972 cm^{-1} in THF). The solution was dried and the solid recrystallized by *n*-hexane–CH_2Cl_2; 4.0 g of 1 (yield 75%) being obtained. Anal. Calcd for $C_8H_{18}Br_2O_2P_2Fe$: C, 22.67; H, 4.28. Found: C, 22.5; H, 4.32.

(b) Method II. $[Fe(CO)_4Br_2]$ (0.5 g) was dissolved in a solution of PMe_3 in diethyl ether. The evolution of carbon monoxide and formation of 1 were immediately observed. The solution was dried and the complex purified as previously described; 0.5 g of 1 was obtained (yield 80%).

$[Fe(CO)_2(PMe_2Ph)_2Br_2]$ (2). Equimolar quantities of $[Fe(CO)_4Br_2]$ (1.0 g) and PMe_2Ph (0.84 g) were dissolved in 100 mL of benzene at 6 °C. The reaction was immediate, and the initial formation of the monosubstituted derivative $[Fe(CO)_3(PMe_2Ph)Br_2]$ (ν_{CO} 2107, 2059, 2028 cm^{-1}) was observed. $[Fe(CO)_3(PMe_2Ph)Br_2]$ quickly transforms into 2 (ν_{CO} 2039, 1976 cm^{-1}), which was purified as 1, giving 1.3 g of the product (yield 80%). Anal. Calcd for $C_{18}H_{22}Br_2O_2P_2Fe$: C, 39.45; H, 4.05. Found: C, 39.6; H, 3.98.

$[Fe(CO)_2(PMePh_2)_2Br_2]$ (3). $[Fe(CO)_4Br_2]$ (1.2 g) was dissolved in 100 mL of benzene. $PMePh_2$ (1.5 g) was dissolved in 10 mL of benzene. The two solutions were mixed at room temperature. After 1 h the reaction was complete. The solution was dried, and the solid residue was crystallized from a *n*-hexane–CH_2Cl_2 mixture. Red-orange crystals (2.2 g of 3) were obtained (yield 80%) (ν_{CO} 2034, 1980 cm^{-1} in CH_2Cl_2). Anal. Calcd for $C_{28}H_{26}Br_2O_2P_2Fe$: C, 50.03; H, 3.90. Found: C, 49.55; H, 4.02.

$[Fe(CO)_2(P(n\text{-}Bu)_3)_2Br_2]$ (4). $[Fe(CO)_4Br_2]$ (1.4 g) was reacted with $P(n\text{-}Bu)_3$ (2 g) in 100 mL of benzene at room temperature. The reaction proceeds in two steps. The first step is instantaneous and gives $[Fe(CO)_3(P(n\text{-}Bu)_3)Br_2]$ (ν_{CO} 2103, 2052, 2018 cm^{-1}). Complex 4 was formed more slowly (1 h). It was crystallized from *n*-hexane–CH_2Cl_2, 2.7 g of red crystals of 4 being obtained (yield 80%) (ν_{CO} 2022, 1969 cm^{-1} in MeCN; 2015, 1963 cm^{-1} in *n*-hexane). Anal. Calcd for $C_{26}H_{54}Br_2O_2P_2Fe$: C, 46.17; H, 8.05. Found: C, 46.30; H, 8.22.

$[Fe(CO)_2(P(i\text{-}Bu)_3)_2Br_2]$ (5). $[Fe(CO)_4Br_2]$ (1.35 g) and $P(i\text{-}Bu)_3$ (1.5 g) were dissolved in 50 mL of benzene. The reaction is fast (0.5 h); vigorous evolution of carbon monoxide was observed. Complex 5 (2.2 g) was obtained by crystallization from *n*-hexane–CH_2Cl_2 as red crystals (yield 80%) (ν_{CO} 2013, 1957 cm^{-1} in *n*-hexane).

$[Fe(CO)_2(P(i\text{-}Pr)_3)_2Br_2]$ (6). $[Fe(CO)_4Br_2]$ (1.5 g) and $P(i\text{-}Pr)_3$ (1.4 g) were reacted in benzene. An initial formation of $[Fe(CO)_3(P(i\text{-}Pr)_3)Br_2]$ (ν_{CO} 2102, 2054, 2022 cm^{-1}) was observed. Slower formation (2 h) of $[Fe(CO)_2(P(i\text{-propyl})_3)_2Br_2]$ (ν_{CO} 2009, 1955 cm^{-1}) and $[Fe(CO)_3(P(i\text{-}Pr)_3)_2]$ (ν_{CO} = 1859 cm^{-1}) was observed. The two complexes were not purified and for the successive reactions were used as a mixture.

$[Fe(CO)_2(P(i\text{-}Pr)_3)_2Cl_2]$ (7). $[Fe(CO)_4Cl_2]$ (0.65 g) and $P(i\text{-}Pr)_3$ (0.8 g) (molar ratio = 1/2) were reacted in benzene solution at room temperature. Complex 7 was formed after 1 h (ν_{CO} 2013, 1956 cm^{-1}). It contained small quantities of $[Fe(CO)_3(P(i\text{-}Pr)_3)_2]$. The formation of the intermediate $[Fe(CO)_3(P(i\text{-}Pr)_3)Br_2]$ was not observed.

$[Fe(CO)_2(PEtPh_2)_2Br_2]$ (8). $[Fe(CO)_4Br_2]$ (2 g) and $PEtPh_2$ (2.6 g) were mixed in benzene at room temperature. After 5 min

(4) Bock, P. L.; Boschetto, D. J.; Rasmussen, J. R.; Demers, J. P.; Whitesides, G. M. *J. Am. Chem. Soc.* **1974**, *96*, 2814–2825.
(5) (a) Pankowski, M.; Bigorgne, M. *J. Organomet. Chem.* **1971**, *30*, 227–234. (b) Reichenbach, G.; Cardaci, G.; Bellachioma, G. *J. Chem. Soc., Dalton Trans.* **1982**, 847–850.
(6) Bellachioma, G.; Cardaci, G.; Reichenbach, G. *J. Chem. Soc., Dalton Trans.* **1983**, 2593–2597.
(7) Jablonski, C. R. *Inorg. Chem.* **1981**, *20*, 3940–3947.
(8) (a) Fachinetti, G.; Floriani, C.; Marchetti, F.; Merlino, S. *J. Chem. Soc., Chem. Commun.* **1976**, 522–523. Fachinetti, G.; Fochi, G.; Floriani, C. *J. Chem. Soc., Dalton Trans.* **1977**, 1946–1950. Fachinetti, G.; Floriani, C.; Stoeckli-Evans, H. *J. Chem. Soc., Dalton Trans.* **1977**, 2297–2302. (b) Roper, W. R.; Taylor, G. E.; Waters, J. M.; Wright, L. J. *J. Organomet. Chem.* **1979**, *182*, C46–C48. (c) Franke, U.; Weiss, E. *J. Organomet. Chem.* **1979**, *165*, 329–340. (d) Fagan, P. J.; Manriquez, J. M.; Marks, T. J.; Day, V. M.; Vollner, S. M.; Day, C. S. *J. Am. Chem. Soc.* **1980**, *102*, 5393–5398. (e) Carmona, E.; Sanchez, L.; Marin, J. M.; Poveda, M. L.; Atwood, J. L.; Priester, R. D.; Rogers, R. D. *J. Am. Chem. Soc.* **1984**, *106*, 3214–3222. (f) Kreisl, F. R.; Sieber, W. J.; Wolfgruber, M.; Riede, J. *Angew. Chem., Int. Ed. Engl.* **1984**, *23*, 640.
(9) Cardaci, G. *Inorg. Chem.* **1974**, *13*, 368–371. Cardaci, G. *Ibid.* **1974**, *13*, 2974–2976. Fischler, I.; Hildebrand, K.; Koerner von Gustorf, E. *Angew. Chem., Int. Ed. Engl.* **1975**, *14*, 54–56.
(10) Hieber, W.; Mushi, J. *Chem. Ber.* **1965**, *98*, 3931–3936.
(11) Bellachioma, G.; Cardaci, G. *Gazz. Chim. Ital.* **1986**, *116*, 475–477.
(12) Coetzee, J. F.; Cunningham, G. P.; McGuire, D. K.; Padmanabham, G. R. *Anal. Chem.* **1962**, *34*, 1139–1143.
(13) Wolfsberger, W.; Schmidbaur, H. *Synth. React. Inorg. Met. Org. Chem.* **1974**, *4*, 149–156.
(14) Cohen, I. A.; Basolo, F. *J. Inorg. Nucl. Chem.* **1966**, *28*, 511–520.
(15) Hieber, W.; Bader, G. *Chem. Ber.* **1928**, *61*, 1717–1722.
(16) Douek, I. C.; Wilkinson, G. *J. Chem. Soc. A* **1969**, 2604–2610.

the formation of $[Fe(CO)_3(PEtPh_2)Br_2]$ (ν_{CO} 2106, 2060, 2033 cm^{-1}) was observed. After 2 h the formation of **8**, too, was complete (ν_{CO} 2034, 1981 cm^{-1}). Complex **8** was purified as **1** and obtained as red crystals (3.7 g) (yield 80%). Anal. Calcd for $C_{30}H_{30}Br_2O_2P_2Fe$: C, 51.46; H, 4.32. Found: C, 51.7; H, 4.15.

$[Fe(CO)_2L_2X_2]$ (L = PPh_3; X = Br (9), Cl (10)). (a) Method I. $[Fe(CO)_3(PPh_3)_2]$ does not react with I_2, Br_2, or Cl_2.

(b) Method II. $[Fe(CO)_4X_2]$ reacts with PPh_3. With X = Br or Cl the reaction gives $[Fe(CO)_2(PPh_3)_2Br_2]$ (**9**) and $[Fe(CO)_2(PPh_3)_2Cl_2]$ (**10**). With X = I the reaction stops with the formation of $[Fe(CO)_3(PPh_3)I_2]$ (ν_{CO} 2088, 2062, 2027 cm^{-1} in benzene).

9: $[Fe(CO)_4Br_2]$ (1 g) and PPh_3 (1.5 g) were dissolved in 100 mL of $CHCl_3$ at room temperature. The formation of $[Fe(CO)_3(PPh_3)Br_2]$ (ν_{CO} 2109, 2063, 2036 cm^{-1}) was immediately observed. It transforms in 0.5 h into complex **9** (ν_{CO} 2038, 1989 cm^{-1}). Small quantities of $[Fe(CO)_3(PPh_3)_2]$ were observed (ν_{CO} 1886 cm^{-1}). **9** was crystallized as previously described and obtained as dark red crystals (2 g) (yield 80%). Anal. Calcd for $C_{34}H_{30}Br_2O_2P_2Fe$: C, 54.58; H, 4.04. Found: C, 54.7; H, 3.87.

10: $[Fe(CO)_4Cl_2]$ (1.3 g) was reacted at 6 °C in benzene with 2.8 g of PPh_3. The reaction is instantaneous, formation of (**10**) being observed (ν_{CO} 2040, 1990 cm^{-1} in MeCN; ν_{CO} 2039, 1988 cm^{-1} in benzene; ν_{CO} 2040, 1980 cm^{-1} in *n*-hexane). Also in this case small quantities of $[Fe(CO)_3(PPh_3)_2]$ were observed. **10** was crystallized as previously described and obtained as yellow crystals (3 g) (yield 70%). Anal. Calcd for $C_{34}H_{30}Cl_2O_2P_2Fe$: C, 61.94; H, 4.59. Found: C, 62.1; H, 4.45.

Reduction and Oxidative Addition. Reduction of 1. **1** (1 g) was dissolved in 25 mL of MeCN at −18 °C. An excess of sodium amalgam (1% of Na) was added. The suspension was stirred for 1.5 h. During the reaction a change in color was observed. The initial orange color changed after 10 min to an emerald green color. Successively a red color was obtained. The color change is related to the formation of complex **1a**, which shows CO stretching frequencies at 1957 and 1870 cm^{-1}. The red color is associated to the formation of the complex $[Fe(CO)_2(PMe_3)_2(MeCN)]$ (**1b**) (ν_{CO} 1852, 1791 cm^{-1}). Complex **1b** was not purified and was used for further reactions in MeCN solution.

Reaction of 1b with CH_3I. To 100 mL of the solution of **1b** in MeCN, thermostated at −15 °C, was added 5 mL of CH_3I. After 5 min the reaction was complete. The IR spectrum showed bands at 2022, 1997, 1966, and 1936 cm^{-1}. The solution was dried, and the residue was dissolved in *n*-hexane. The IR spectrum showed bands at 2002 and 1943 cm^{-1}. Crystallization from *n*-hexane solution gave red crystals of $[Fe(CO)_2(PMe_3)_2(CH_3)I]$ (**1c**). Yield with respect to complex **1**: 70%. Anal. Calcd for $C_9H_{21}IO_2P_2Fe$: C, 26.63; H, 5.21. Found: C, 26.5; H, 5.31.

Reaction of 1b with C_2H_5I. To 100 mL of the solution of **1b** in MeCN, kept at −18 °C, was added 7 mL of C_2H_5I. At this temperature the reaction did not occur. The temperature was raised to 20 °C, and the reaction was complete in 1 h. The MeCN solution showed bands at 1937 and 1595 cm^{-1}. The solution was dried with an oil pump. The residue was dissolved in diethyl ether and the solution filtered. The solution showed bands at 1993 and 1933 cm^{-1}, corresponding to the complex $[Fe(CO)_2(PMe_3)_2(C_2H_5)I]$ (**1c′**). Red crystals of **1c′** were obtained from a *n*-hexane solution at −18 °C (ν_{CO} 1995, 1935 cm^{-1}). Yield with respect to complex **1**: 40%. Anal. Calcd as $C_{10}H_{23}IO_2P_2Fe$: C, 28.60; H, 5.52. Found: C, 28.9; H, 5.45.

Reaction of 1b with $C_6H_5CH_2Br$. To 100 mL of a solution of **1b** in MeCN, kept at −20 °C, was added 20 mL of $C_6H_5CH_2Br$. The reaction is fast and the initial formation of a complex (ν_{CO} 2000, 1937 cm^{-1}), having the probable structure $[Fe(CO)_2(PMe_3)_2(C_6H_5CH_2)Br]$ (**1c″**), was observed. This complex is unstable and reacts with the excess of $C_6H_5CH_2Br$, re-forming complex **1** (ν_{CO} 2028, 1976 cm^{-1}).

Reduction of 2 and Oxidative Addition with CH_3I. Complex **2** (5.5 g) was dissolved in 100 mL of MeCN and the solution cooled to −20 °C. An excess of sodium amalgam (1%) was added, and the suspension was stirred vigorously. The solution changed immediately from orange to green (ν_{CO} 1961, 1871 cm^{-1}) (complex **2a**). After 15 min the color changed to red, and after 2 h the reaction was complete with formation of complex **2b** (ν_{CO} 1856, 1799 cm^{-1}). The solution was filtered and kept at 0 °C. CH_3I (5 mL) was added. After 3 min the IR spectrum showed bands at 2025, 2001, 1970, and 1940 cm^{-1}. The solution was dried and the solid residue was dissolved in *n*-hexane (ν_{CO} 2005, 1941 cm^{-1}). Complex $[Fe(CO)_2(PMe_2Ph)_2(CH_3)I]$ (**2c**) was obtained from this solution at −18 °C as red crystals. Yield with respect to complex **2**: 70%. Anal. Calcd as $C_{19}H_{25}IO_2P_2Fe$: C, 43.05; H, 4.75. Found: C, 42.8; H, 4.95.

Reduction of 3 and Oxidative Addition with CH_3I. Complex **3** (6.8 g) was dissolved in 150 mL of MeCN and the solution kept at −20 °C. At this temperature the complex was not completely dissolved and a suspension was obtained. Sodium amalgam was added, and the solution was stirred vigorously. The course of the reaction was as for the previous complexes, but the reaction time was about 3 h because complex is only slightly soluble in MeCN. The green complex **3a** showed bands at 1964 and 1887 cm^{-1}, and the final red solution of **3b** showed CO bands at 1862 and 1803 cm^{-1}. The solution was filtered and kept at −10 °C. It showed an equilibrium between complexes **3a** and **3b**. CH_3I (20 mL) was added. The reaction continued for 5 h under vigorous stirring. The solution was dried, and the solid was crystallized from CH_2Cl_2. Well-formed dark red crystals of $[Fe(CO)(PMePh_2)_2(\eta^2\text{-}COCH_3)I]\cdot 2CH_2Cl_2$ (**3d**) were obtained (yield with respect to complex **3**: 40%). Anal. Calcd for $C_{31}H_{33}Cl_4IO_2P_2Fe$: C, 45.18; H, 4.04. Found: C, 45.3; H, 4.0. The IR spectrum showed the following bands (cm^{-1}): in fluorolube, ν_{CO} 1904; ν_{COMe} 1578; in CH_2Cl_2, ν_{CO} 1902, ν_{COMe} 1587; in KBr, ν_{CO} 1906, ν_{COMe} 1572, 1577; in Nujol, ν_{CO} 1904, ν_{COMe} = 1571, 1579.

Reduction of 4 and Oxidative Addition with CH_3I. Complex **4** was dissolved in MeCN and kept at −20 °C. Sodium amalgam was added, and the solution was stirred. After 15 min the color changed from orange to green with formation of complex **4a**: ν_{CO} 1950, 1875 cm^{-1}. After 30 min the color changed to red with the formation of complex **4b**: ν_{CO} 1847, 1781 cm^{-1}. Even after 3 h complex **4a** did not disappear, and on raising the temperature (20 °C), its relative intensity increased, indicating an equilibrium with complex **4b**. The equilibrium mixture was used for the further reactions.

To this solution, kept at −20 °C, was added 5 mL of CH_3I. An immediate reaction was observed with the formation of a complex having CO bands at 2013 and 1959 cm^{-1}. The solution was dried, and the solid dissolved in *n*-hexane: ν_{CO} 1989, 1928 cm^{-1}. Complex $[Fe(CO)_2(P(n\text{-}Bu)_3)_2(CH_3)I]$ (**4c**) was obtained as red crystals from this solution, kept at −20 °C (yield with respect to complex **4**: 70%). Anal. Calcd for $C_{27}H_{57}IO_2P_2Fe$: C, 49.25; H, 8.73. Found: C, 49.1; H, 8.85.

Reduction of 5. Complex **5** (2 g) was dissolved in MeCN and cooled at −20 °C. Sodium amalgam was added, and the solution was stirred. The formation of complex **5a** was immediately observed: ν_{CO} 1949, 1873 cm^{-1}. After 40 min the formation of complex **5b** was observed: ν_{CO} 1853, 1783 cm^{-1}. Complexes **5a** and **5b** are in equilibrium, the equilibrium being shifted toward **5a** at room temperature. The emerald green solution at room temperature was dried and the solid dissolved in *n*-hexane: ν_{CO} 1969, 1871 cm^{-1}. Many attempts were performed to crystallize complex **5a**, but, owing to its high solubility in *n*-hexane and in the other common solvents and to its reactivity with oxygen, it was not possible to obtain it in the crystalline form.

Reaction of 5a and 5b with CH_3I. To 100 mL of the MeCN solution of **5a** and **5b** in equilibrium, kept at −20 °C, was added 10 mL of CH_3I. The reaction was very slow, so the temperature was raised at 20 °C. After 2 h the reaction was complete. The formation of complex $[Fe(CO)(P(i\text{-}Bu)_3)_2(\eta^2\text{-}COCH_3)I]$ (**5d**) was observed: ν_{CO} 1894 cm^{-1}, ν_{COMe} 1603 cm^{-1} in *n*-hexane. Attempts to crystallize complex **5d** were unsuccessful because of its high solubility.

Reaction of 5a and 5b with C_2H_2I. To 100 mL of the MeCN solution of **5a**, kept at −20 °C, was added 15 mL of C_2H_5I. After 3 h, the reaction was complete and complex $[Fe(CO)(P(i\text{-}Bu)_3)_2(\eta^2\text{-}COC_2H_5)I]$ (**5d′**) was obtained: ν_{CO} 1893 cm^{-1}, ν_{COEt} 1606 cm^{-1} in *n*-hexane. Neither in this case could complex **5d′** be obtained in crystalline form for analytical characterization.

Reduction of 6 and 7. The mixture of **6** or **7** and $[Fe(CO)_3(P(i\text{-}Pr)_3)_2]$ was used without further purification. The mixture (2 g) was dissolved in MeCN and kept at −20 °C. After addition of sodium amalgam and stirring (50 min) the reduction was complete and formation of complex **6a** was observed: ν_{CO} 1950, 1871 cm^{-1}. No formation of complex $[Fe(CO)_2(P(i\text{-}Pr)_3)_2(MeCN)]$ (**6b**) was observed. To the solution of (**6a**) was added

CH_3I. Decomposition of the complex was observed.

Reduction of 8. Complex 8 (2 g) was dissolved in 100 mL of MeCN and kept at −10 °C. After addition of sodium amalgam, the solution was vigorously stirred. Complex **8a** was observed after 55 min of reaction: ν_{CO} 1964, 1885 cm^{-1}. The reaction was complete after 4 h with formation of complex $[Fe(CO)_2(PEtPh_2)_2(MeCN)]$ (**8b**): ν_{CO} 1862, 1803 cm^{-1}. The solution was cleared and separated from the precipitate. To this solution, kept at −10 °C, was added 20 mL of CH_3I. After 6 h the reaction was complete and formation of $[Fe(CO)(PEtPh_2)_2(\eta^2\text{-}COCH_3)I]$ was obtained: ν_{CO} 1903 cm^{-1}; ν_{COMe} 1592 cm^{-1}. The solution was dried, and complex **8d** crystallized from CH_2Cl_2 as dark red crystals. $[Fe(CO)(PEtPh_2)_2(\eta^2\text{-}COCH_3)I\cdot 2CH_2Cl_2]$ (**8d**) (ν_{CO} 1901 cm^{-1}, ν_{COMe} 1587 cm^{-1} in CH_2Cl_2) was obtained. Yield with respect to complex 8: 40%. Anal. Calcd for $C_{31}H_{33}IO_2P_2Fe$: C, 54.57; H, 4.87. Found: C, 54.7; H, 4.95.

Reduction of 10. Complex **9** was not reduced by sodium amalgam in MeCN, owing to its insolubility in this solvent. Complex **10** is slightly more soluble in MeCN, and its reduction in MeCN was possible.

Complex **10** (2 g) was dispersed in 150 mL of MeCN and kept at −20 °C. Sodium amalgam was added, and the solution was stirred vigorously. After 10 h the reaction was complete, and the formation of complex $[Fe(CO)_2(PPh_3)_2(MeCN)]$ (**9b**) (ν_{CO} 1863, 1804 cm^{-1}) was observed in solution. The greater part of the reduction product is present as complex **9a** in the solid suspension: ν_{CO} 1956, 1882 cm^{-1}. If the reduction of **10** is carried in diethyl ether, the formation of a product, showing CO bands at 1888 and 1836 cm^{-1}, is observed. This complex may be the trisubstituted complex $[Fe(CO)_2(PPh_3)_2(Et_2O)]$.

Reaction of 9a with CH_3I. Complex **9a**, obtained by drying the solution containing the reduction in MeCN, was reacted with CH_3I, and complex $[Fe(CO)(PPh_3)_2(\eta^2\text{-}COCH_3)I]$ (**9d**) was immediately obtained. It was crystallized from CH_2Cl_2–*n*-hexane. Yield with respect to complex **10**: 20% (ν_{CO} 1904 cm^{-1}, ν_{COMe} 1589 cm^{-1} in CH_3I; ν_{CO} 1904 cm^{-1}, ν_{COMe} 1591 cm^{-1} in CH_2Cl_2; ν_{CO} 1886 cm^{-1} ν_{COMe} 1854 cm^{-1} in fluorolube). Anal. Calcd for $C_{39}H_{33}IO_2P_2Fe$: C, 60.18; H, 4.27. Found: C, 60.3; H, 4.35.

Reduction of 5 in diethyl ether. A solution of **5** (1 g) in diethyl ether was reduced at −30 °C with sodium amalgam. The reaction was complete after 70 min. The emerald green solution was filtered and kept at room temperature. The complex obtained was stable in solution and showed CO stretching frequencies at 1950 and 1878 cm^{-1}. Its structure may be **5a** (Figure 1).

Collection of X-ray Diffraction Data for Complex 3d. A dark red crystal of **3d** was used for the determination of cell parameters and subsequent data collection. The crystal was mounted on a glass fiber with epoxy and transferred to the diffractometer. The crystal survey, unit-cell dimension determination, and data were collected at room temperature on a computer-controlled Philips PW 1100 single-crystal diffractometer equipped with graphite-monochromated Mo Kα radiation (λ = 0.71069 Å). The observed systematic absences are consistent with the monoclinic space group $P2_1/n$. Cell dimensions were determined from a least-squares refinement based on the setting angles of 25 reflections with 2θ ranging between 17° and 22°.

The intensities were collected up to 2θ = 50°. A total of 6650 independent reflections were measured, of which 4008 having $I < 3\sigma(I)$ were considered as "unobserved" and excluded from the refinement. Three standard reflections, measured periodically, showed no apparent variation in intensity during data collection. The linear absorption coefficient for Mo Kα radiation is μ = 16.2 cm^{-1}. The data were corrected for Lorentz and polarization factors. A semiempirical absorption correction was applied on the basis of the variation in intensity during the azimuthal scans of some reflections according to the method of North et al.;[17] the transmission factors were in the range 0.95–0.75.

The structure was solved by the direct method and refined by the full-matrix least-squares method with the SHELX-76 package of programs.[18] During the refinement a difference Fourier synthesis showed some residual maxima of electron density ascribable to molecules of CH_2Cl_2 used as solvent. The phenyl groups were constrained to perfect hexagons (C–C = 1.395 Å) and refined as rigid groups, with individual isotropic thermal parameters assigned to each C atom. The hydrogen atoms (with the exception of those of the methyl groups and of the solvent molecules) were included at the calculated positions with overall isotropic parameter of U = 0.13 $Å^2$. Anisotropic thermal parameters were refined for Fe, I, Cl, and P atoms. The high values of thermal parameters assumed by chlorine and C atoms of the CH_2Cl_2 solvent molecules are probably indicative of partially occupancy. The refinement converged at R(unweighted) = 0.058 and R(weighted) = 0.062 for 159 parameters and 2642 observed reflections ($R_w = (\sum w(|F_o| - |F_c|)^2)^{1/2}$, $w = (\sigma^2(F_o) + 0.0023F_o^2)^{-1}$).

The atomic scattering factors were taken from ref 18 for P, O, N, C, Cl, and H and from ref 19 for Fe and I: The correction for anomalous dispersion was included. A summary of crystal data and intensity collection are given in Table I. The atomic coordinates are listed in Table II. Relevant bond distances (Å) and angles (deg) are given in Table III.

Table I. Summary of Crystal Data and Intensity Collection for Complex 3d

A. Crystal Data	
formula	$C_{29}H_{29}IO_2P_2Fe\cdot 2CH_2Cl_2$
cryst dimens, mm	0.49 × 0.34 × 0.15
color	dark red
cell params (errors)	
a, Å	23.603 (4)
b, Å	12.256 (3)
c, Å	12.318 (3)
β, deg	97.08 (2)
cryst type	monoclinic
space group	$P2_1/n$
Z	4
d(calcd), g/cm^3	1.546
B. Data Collection and Reduction	
diffractometer	Philips PW1100
monochromator	graphite
radiatn	Mo Kα (λ = 0.71069 Å)
temp, °C	20
scan range, deg	$2\theta \leq 50$
scan method	ω–2θ
scan width, deg	1.4
scan speed, deg s^{-1}	0.05
μ, cm^{-1}	16.2
abs corrtn	empirical
no. of unique data	6650
no. of data with $I > 3\sigma(I)$	2642
T_{min}, T_{max}	0.75, 0.95
C. Solution and Refinement	
R	0.058
R_w	0.062

Results

(1) Complexes $[Fe(CO)_2L_2X_2]$. Complexes $[Fe(CO)_2L_2X_2]$ can be prepared following two methods: the first method is the oxidative addition of a halogen to the disubstituted derivatives of iron pentacarbonyl $[Fe(CO)_3L_2]$. This method, already described in the literature,[20] was used with the less bulky and the most basic ligands (viz., PMe_3 etc.) and with I_2. The second method is the substitution of carbon monoxide with phosphine ligands in the complexes $[Fe(CO)_4X_2]$ (X = Cl, Br, I), used by Basolo et al.[14] With X = I the disubstitution reaction does not occur when the cone angle of the phosphine ligands[21] is more than 143°. With X = Br the disubstitution does not occur when the cone angle of L is more than 160°.

(17) North, A. C. T.; Phillips, D. L.; Mathews, F. S. *Acta Crystallogr., Sect. A: Cryst. Phys., Diffr., Theor. Gen. Crystallogr.* **1968**, *A24*, 351–359.
(18) Sheldrick, G. M. *Shelx, Programme for Crystal Structure Determination*: University of Cambridge: Cambridge, England, 1976.
(19) *International Tables of X-ray Crystallography*; Kynoch: Birmingham, England, 1974.
(20) Pankowski, M.; Bigorgne, M. *J. Organomet. Chem.* **1977**, *125*, 231–252.
(21) Tolman, C. A. *Chem. Rev.* **1977**, *77*, 313–348.

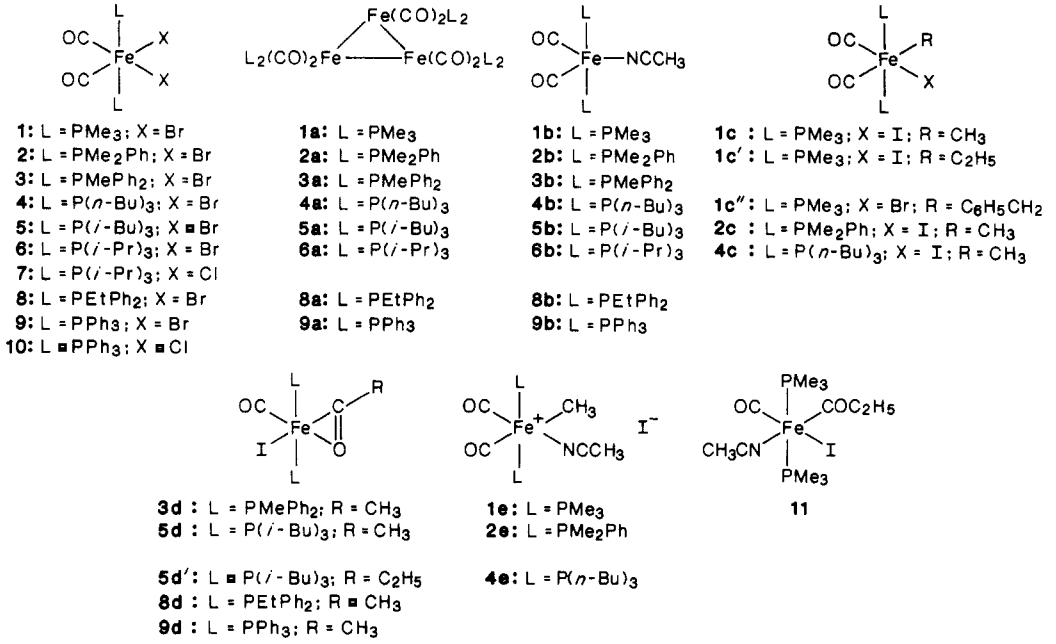

Figure 1. View of the structure of the complexes.

Scheme I

$$3Fe(CO)_2L_2X + Na/Hg \xrightarrow[T = -20/0\ ^\circ C]{MeCN} [Fe(CO)_2L_2]_3 \quad (1a)$$

$$[Fe(CO)_2L_2]_3 \underset{T = -20/0\ ^\circ C}{\overset{MeCN}{\rightleftharpoons}} 3Fe(CO)_2L_2(MeCN) \quad (1b)$$

With L = $P(C_6H_{11})_3$ only the monosubstituted complex $[Fe(CO)_3(P(C_6H_{11})_3)X_2]$ was obtained. With a cone angle more than 142°, partial reductive elimination of X_2 was observed with the formation of the disubstituted derivatives $[Fe(CO)_3L_2]$.

The structure of the disubstituted derivatives $[Fe(CO)_2L_2X_2]$ is shown in Figure 1. It was ascertained on the basis of the IR spectrum, which shows two CO stretching frequencies of equal intensity, and on the basis of the ^1H NMR spectrum of $[Fe(CO)_2(PMe_3)_2Br_2]$, which shows a triplet for the PMe_3 groups (τ 8.23 (J = 4.2 Hz) in CD_2Cl_2). These results are in agreement with two CO groups in the cis position and with two PMe_3 groups in the trans position.[22] The structure ascertained for complex **1** was assumed for all the other dihalide complexes, which show similar IR spectra.

(2) Reduction of $[Fe(CO)_2L_2X_2]$. The general picture of the reduction of complexes $[Fe(CO)_2L_2X_2]$ with sodium amalgam in MeCN is given in Scheme I. The reaction occurs in two steps with the formation of the first intermediate $[Fe(CO)_2L_2]_3$, followed by a second equilibrium step, which gives $[Fe(CO)_2L_2(MeCN)]$. For the occurrence of the second step MeCN is necessary. The first step also occurs with other solvents (viz., diethyl ether). Equilibrium 1b is shifted toward $[Fe(CO)_2L_2(MeCN)]$ on decreasing the temperature and steric hindrance of L. At room temperature with L = P(i-Bu)$_3$ the equilibrium is shifted completely toward $[Fe(CO)_2(P(i\text{-}Bu)_3)_2]_3$ (**5a**). Many attempts to obtain **5a** in crystalline form were unsuccessful, owing to its high solubility in organic solvents and to its oxygen reactivity. The spectroscopic information does not resolve the structure of the $[Fe(CO)_2L_2]_3$ complexes; it has been assigned on the basis of the course of the reaction and of the similarity with the visible spectrum of $[Fe_3(CO)_{12}]$.

(22) Jenkins, J. M.; Shaw, B. L. *J. Chem. Soc. A* **1966**, 1407–1409.
(23) Bruce, M. I.; Matisons, J. G.; Skelton, B. W.; White, A. H. *J. Chem. Soc., Dalton Trans.* **1983**, 2375–2384.

Table II. Fractional Atomic Coordinates in Complex 3d[a]

atom	x/a	y/b	z/c
I	0.1529	0.1144 (1)	0.1702 (1)
Fe	0.1356 (1)	0.3209 (1)	0.1030 (1)
P(1)	0.1365 (1)	0.3761 (2)	0.2783 (2)
P(2)	0.1380 (1)	0.2668 (2)	−0.0725 (3)
O(1)	0.0194 (4)	0.3903 (7)	0.0554 (7)
O(2)	0.2219 (4)	0.3983 (7)	0.1010 (7)
C(1)	0.0667 (5)	0.3613 (9)	0.0755 (9)
C(2)	0.1755 (5)	0.4436 (9)	0.0758 (9)
C(3)	0.1674 (5)	0.5608 (10)	0.0400 (10)
C(4)	0.2045 (6)	0.1929 (10)	−0.0964 (10)
C(5)	0.1356 (3)	0.3810 (5)	−0.1691 (6)
C(6)	0.1824 (3)	0.4101 (5)	−0.2220 (6)
C(7)	0.1791 (3)	0.5011 (5)	−0.2906 (6)
C(8)	0.1292 (3)	0.5629 (5)	−0.3063 (6)
C(9)	0.0824 (3)	0.5338 (5)	−0.2533 (6)
C(10)	0.0857 (3)	0.4429 (5)	−0.1847 (6)
C(11)	0.0809 (3)	0.1783 (6)	−0.1380 (5)
C(12)	0.0798 (3)	0.1528 (6)	−0.2486 (5)
C(13)	0.0366 (3)	0.0861 (6)	−0.3000 (5)
C(14)	−0.0054 (3)	0.0450 (6)	−0.2408 (5)
C(15)	−0.0042 (3)	0.0706 (6)	−0.1302 (5)
C(16)	0.0389 (3)	0.1372 (6)	−0.0788 (5)
C(17)	0.2041 (6)	0.3412 (12)	0.3665 (11)
C(18)	0.0798 (3)	0.3301 (6)	0.3558 (6)
C(19)	0.0395 (3)	0.2532 (6)	0.3132 (6)
C(20)	−0.0045 (3)	0.2229 (6)	0.3729 (6)
C(21)	−0.0081 (3)	0.2693 (6)	0.4752 (6)
C(22)	0.0322 (3)	0.3461 (6)	0.5178 (6)
C(23)	0.0762 (3)	0.3765 (6)	0.4581 (6)
C(24)	0.1306 (3)	0.5237 (4)	0.2919 (7)
C(25)	0.0784 (3)	0.5723 (4)	0.2550 (7)
C(26)	0.0738 (3)	0.6857 (4)	0.2504 (7)
C(27)	0.1214 (3)	0.7505 (4)	0.2829 (7)
C(28)	0.1737 (3)	0.7019 (4)	0.3199 (7)
C(29)	0.1783 (3)	0.5885 (4)	0.3244 (7)
C(30)	0.3672 (11)	0.3904 (19)	0.5805 (19)
C(31)	0.1593 (11)	0.0244 (21)	0.4780 (19)
Cl(1)	0.4198 (2)	0.2931 (4)	0.5800 (5)
Cl(2)	0.3071 (3)	0.3483 (7)	0.6261 (7)
Cl(3)	0.1941 (3)	0.1164 (6)	0.5727 (6)
Cl(4)	0.1376 (5)	−0.0863 (9)	0.5475 (10)

[a] Esd's in parentheses refer to the last digit.

The formation in different solvents, some of which having little affinity with the iron atom (viz., diethyl ether), suggests that the solvent is absent in the molecular structure of $[Fe(CO)_2L_2]_3$. The IR spectrum shows two CO

Table III. Relevant Bond Distances (Å) and Angles (deg) for Complex 3d[a]

		Bond Distances			
I–Fe	2.678 (2)	Fe–O(2)	2.250 (9)	O(1)–C(1)	1.169 (13)
Fe–P(1)	2.260 (3)	Fe–C(2)	1.827 (11)	O(2)–C(2)	1.233 (14)
Fe–P(2)	2.269 (4)	Fe–C(1)	1.694 (11)	C(2)–C(3)	1.508 (16)
		Bond Angles			
I–Fe–P(1)	90.3 (1)	P(1)–Fe–C(2)	89.1 (3)	C(2)–Fe–C(1)	103.1 (5)
I–Fe–P(2)	89.9 (1)	P(1)–Fe–C(1)	90.0 (4)	Fe–C(1)–O(1)	179.0 (10)
I–Fe–O(2)	107.3 (2)	P(2)–Fe–O(2)	89.1 (2)	Fe–O(2)–C(2)	54.2 (6)
I–Fe–C(2)	140.5 (3)	P(2)–Fe–C(2)	89.5 (3)	Fe–C(2)–O(2)	92.6 (7)
I–Fe–C(1)	116.4 (4)	P(2)–Fe–C(1)	91.8 (4)	Fe–C(2)–C(3)	142.0 (8)
P(1)–Fe–P(2)	178.0 (1)	O(2)–Fe–C(2)	33.2 (4)	O(2)–C(2)–C(3)	125.4 (10)
P(1)–Fe–O(2)	89.0 (2)	O(2)–Fe–C(1)	136.3 (4)		

[a] Esd's in parentheses refer to the last digit.

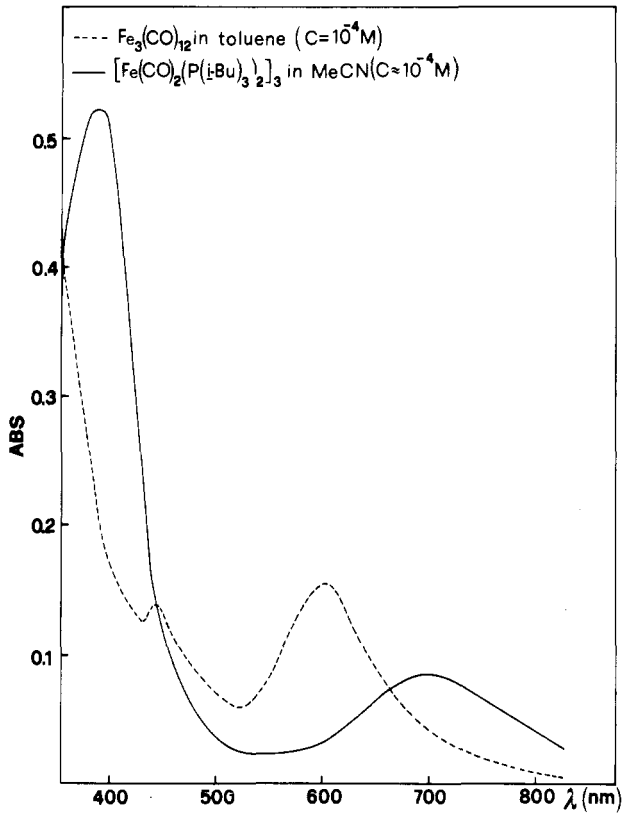

Figure 2. Visible spectrum of $Fe_3(CO)_{12}$ in toluene (- - -) and visible spectrum of $[Fe(CO)_2(P(i\text{-}Bu)_3)_2]_3$ in MeCN (—).

stretching frequencies in the range 1970–1860 cm^{-1}. The visible spectrum of $[Fe(CO)_2(P(i\text{-}Bu)_3)_2]_3$ in MeCN shows a band at the lowest energy (λ_{max} 695 nm) compared with the band at the lowest energy for $Fe_3(CO)_{12}$ (λ_{max} 600 nm in toluene) (Figure 2). This large bathochromic effect by substitution of CO ligands with phosphine ligands has also been observed in the series $[Ru_3(CO)_{12}]$ (λ_{max} 390 nm in 2-methylpentane) and $[Ru(CO)_3L]_3$ (λ_{max} 500 nm in 2-methylpentane).[24] This band was assigned in the series $[M_3(CO)_{12}]$ (M = Fe, Ru, Os)[24] to the triangular moiety. The similar behavior observed in the complexes of Fe and Ru supports the cluster structure for the $[Fe(CO)_2L_2]_3$ complexes (Figure 1) without any CO bridge, owing to the absence of CO stretchings assignable to this structure.

The reaction course, too, suggests this structure. The $[Fe(CO)_2L_2]$ product of the reduction[10] can be blocked by MeCN to give $[Fe(CO)_2L_2(MeCN)]$ or trimerize to give $[Fe(CO)_2L_2]_3$ as occurs with the unsaturated species $[Fe(CO)_4]$.[25] The possibility of dimerization to give $[Fe(CO)_2L_2]_2$, similar to the hypothesized $[Fe_2(CO)_8]$ species,[26] electronically equivalent to $CH_2{=}CH_2$,[27] is less probable, owing to its high reactivity.

The structure of $[Fe(CO)_2L_2(MeCN)]$ complexes, shown in Figure 1, has been ascertained for complex **1b** with L = PMe_3. The ^1H NMR spectrum of **1b** shows a triplet for the PMe_3 groups (τ 8.59 (J = 3.75 Hz) in CD_3CN).[22] The two PMe_3 ligands therefore occupy the two trans positions of the trigonal-bipyramidal structure. Consequently, the MeCN ligand occupies a coordination position of the plane of the bipyramid. The structure ascertained for **1b** was assigned by similarity to the other complexes of this type. All these complexes show two CO stretching bands in the range 1780–1865 cm^{-1}, about 50 cm^{-1} lower than the trisubstituted derivatives of $[Fe(CO)_5]$ with phosphine ligands $[Fe(CO)_2L_3]$, which show the same structure:[10] $[Fe(CO)_2(PMe_3)_3]$, ν_{CO} 1835, 1895 cm^{-1} in *n*-pentane,[28] $[Fe(CO)_2(PPh_3)_3]$, ν_{CO} 1840, 1900 cm^{-1} in Nujol;[29] $[Fe(CO)_2(Diphosph)(PPh_3)]$, ν_{CO} 1847, 1904 cm^{-1} in *n*-hexane.[30] The strong effect of MeCN on the CO stretching frequencies can be explained by the small back-bonding toward this ligand, which increases the back-bonding toward the CO ligands, weakening the C–O bond and the CO stretching frequencies, in agreement with the fact that the P-type ligands are better π-bonders than the N-type ligands.[31]

The nature of the L ligands has a smaller effect on the CO stretching fequencies (about 20 cm^{-1}). More basic ligands shift the CO stretching frequencies to lower values, in agreement with an increase of electronic density on the metal.

(3) Oxidative Addition. The labile nature of the Fe–NCMe bond in the $[Fe(CO)_2L_2(MeCN)]$ complexes permits easy dissociation of the bond and allows us to obtain the reactive intermediate $[Fe(CO)_2L_2]$. This same intermediate can be obtained by dissociation of the cluster $[Fe(CO)_2L_2]_3$. Therefore both the species of equilibrium 1b, discussed previously, are reactive to oxidative addition.

The course of the reaction differs according to the nature of L and RI.

(24) Tyler, D. R.; Levenson, R. A.; Gray, H. B. *J. Am. Chem. Soc.* **1978**, *100*, 7888–7893. Graff, J. L.; Sanner, R. D.; Wrighton, M. S. *J. Am. Chem. Soc.* **1979**, *101*, 273–275.

(25) Poliakoff, M.; Turner, J. J. *J. Chem. Soc., Chem. Commun.* **1970**, 1005.

(26) Poliakoff, M.; Turner J. J. *J. Chem. Soc. A* **1971**, 2403–2410.

(27) Hoffmann, R. *Angew. Chem., Int. Ed. Engl.* **1982**, *21*, 711–724.

(28) Harris, T. V.; Rathke, J. W.; Muetterties, E. L. *J. Am. Chem. Soc.* **1978**, *100*, 6966–6977.

(29) Cenini, S.; Porta, F.; Pizzotti, M. *Inorg. Chim. Acta* **1976**, *20*, 119–126.

(30) Bellachioma, G.; Cardaci, G. *J. Organomet. Chem.* **1981**, *205*, 91–98.

(31) Basolo, F.; Pearson, R. G. *Mechanisms of Inorganic Reactions*, 2nd ed.; Wiley: New York, 1967; p 566.

Table IV. IR and ^{1}H NMR Spectra of the Alkyl and η^2-Acyl Complexes

L	ϕ^a	complex	ν_{CO}[b]	ν_{COR}	τ[b]	J, Hz	assignt
PMe_3	118	1c	2002, 1940		9.64 (t)	9.1	Fe-CH_3
					8.38 (t)	4.1	PMe_3
PMe_3	118	1c′	1982, 1943		9.20 (t)	7.0	CH_3-CH_2-Fe
					7.98 (m)	4.0	CH_3-CH_2-Fe
					8.33 (t)		PMe_3
PMe_2Ph	122	2c	2005, 1949		9.41 (t)	8.6	Fe-CH_3
					7.97 (t)	6.0	PMe_2Ph
					8.11 (t)		PMe_2Ph
					2.32–2.79		PMe_2Ph
P(n-Bu)$_3$	132	4c	1980, 1928		9.70 (t)	8.6	Fe-CH_3
					9.05, 8.67, 8.05		P(n-Bu)$_3$
$PMePh_2$	136	3d	1898[c]	1587[c]	8.88 (s)		$COCH_3$
					7.76 (t)		PMePh$_2$
					2.25–2.76		PMePh_2
$PEtPh_2$	140	8d	1901[c]	1587[c]	8.88 (s)	J_{Me-P} = 15.5	$COCH_3$
					8.97 (dt)	J_{Et} = 7.8	$PPh_2CH_2CH_3$
					7.25 (m)		$PPh_2CH_2CH_3$
					2.3–2.8		$PPh_2CH_2CH_3$
P(i-Bu)$_3$	143	5d	1894[c]	1601[c]	8.82 (s)		$COCH_3$
					7.89, 8.82, 8.90		P(i-Bu)$_3$
P(i-Bu)$_3$	143	5d	1893[c]	1605[c]			
PPh_3	145	9d	1904[c]	1588[c]	8.78 (s)		$COCH_3$
					2.25–2.8		PPh_3

[a] Cone angle.[21] [b] IR spectra were performed in n-hexane; ^{1}H NMR spectra in CD_2Cl_2. Abbrevations: t, triplet; s, singlet; dt, double triplet; m, multiplet. [c] IR spectra were performed in CH_2Cl_2.

(a) L = PMe_3, PMe_2Ph, or P(n-Bu)$_3$; R = CH_3. The reaction proceeds following Scheme II.

Scheme II

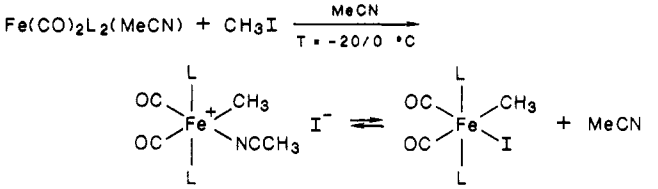

The oxidative addition of CH_3I gives an equilibrium between the ionic complex $[Fe(CO)_2L_2(MeCN)(CH_3)]I$ and the nonionic alkyl complex $[Fe(CO)_2L_2(CH_3)I]$. The equilibrium is shifted toward the ionic species when L = P(n-Bu)$_3$. This equilibrium has already studied for L = PMe_3.[6] The order of increase of the ionic product is P(n-Bu)$_3$ > PMe_2Ph > PMe_3, in agreement with the increase in the steric hindrance of the phosphine ligands. On increasing the steric hindrance, the iodide dissociates and the ionic form is stabilized. Elimination of the MeCN solvent by pumping shifts the equilibrium toward the alkyl complex.

The structure of the alkyl complexes was assigned on the basis of the CO stretching bands and of the ^{1}H NMR spectra (Table IV) as discussed previously for the PMe_3 iron complex[5b] and for similar complexes of ruthenium.[32]

(b) L = PMe_3; R = C_2H_5. The reaction follows Scheme III.

Scheme III

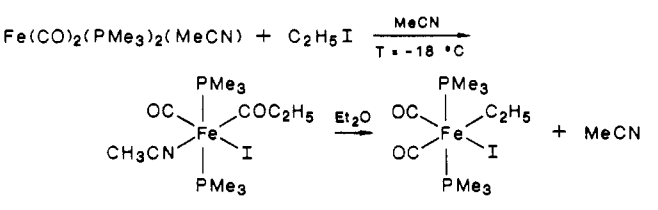

11

The oxidative addition does not give an ionic product, but complex 11 was obtained. It shows a CO stretching band at 1917 cm^{-1} and a $COCH_3$ band at 1595 cm^{-1}. The position of the MeCN ligand in structure 11 is assigned by comparison with the corresponding phosphine derivatives $[Fe(CO)(PMe_3)_2L(COMe)X]$ with L = $P(OMe)_3$, PMe_3 and X = I and CN, discussed previously.[32] Elimination of MeCN solvent by pumping and dissolution in diethyl ether gives the ethyl complex 1c′. In this case, too, the structure was assigned on the basis of the IR and ^{1}H NMR spectra (Table IV).[32]

(c) L = PMe_3; RX = $C_6H_5CH_2Br$. Complex 1b reacts quickly with $C_6H_5CH_2Br$ and gives the alkyl complex 1c″. Owing to the excess of $C_6H_5CH_2Br$ 1c″ is unstable and reacts to give complex 1. This reaction can occur via a radical mechanism, which breaks the iron–benzyl bond, as observed in other complexes containing the benzyl ligand.[33] The structure of 1c″ was assigned only on the basis of the IR spectrum. Its reactivity prevents us from obtaining the ^{1}H NMR spectrum.

(d) L = $PMePh_2$, $PEtPh_2$, P(i-Bu)$_3$, or PPh_3; R = CH_3 or C_2H_5. When the steric hindrance of the phosphine ligands is greater than 135°, the products of the oxidative addition are the η^2-acyl structures $[Fe(CO)L_2(\eta^2\text{-}COR)I]$. In the case of complex 3d the structure was determined by single-crystal X-ray measurements (see below). In the other cases the structure was assigned on the basis of the IR and ^{1}H NMR spectra (Table IV). All these complexes show a CO stretching band at about 1900 cm^{-1} and a COR band at 1590 cm^{-1} in agreement with those of the similar complexes of ruthenium described by Roper et al.[34] The ^{1}H NMR spectra show a η^2-acyl band at τ 8.9 (Table IV). This band is little influenced by the properties of the phosphine ligands, contrary to what is observed in the η^1-acyl groups.[35] This may be due to the fact that electronic effects compensate across the η^2-acyl structures. The chemical shift of this band is very high with respect to the η^1 structure (τ 7.5).[5b,35] The shielding effect of the η^2 structure is higher than that of the η^1 structure, indicating a flux of electron density toward the $COCH_3$ group from the metal.

(32) Barnard, C. F. J.; Daniels, J. A.; Mawby, R. J. *J. Chem. Soc., Dalton Trans.* **1976**, 961–966.
(33) Kochi, J. K. *Organometallic Mechanisms and Catalysis*; Academic: New York, 1978; pp 363–367.
(34) Roper, W. R.; Wright, L. J. *J. Organomet. Chem.* **1977**, *142*, C1–C6.
(35) Barnard, C. F. J.; Daniels, J. A.; Mawby, R. J. *J. Chem. Soc., Dalton Trans.* **1979**, 1331–1338.

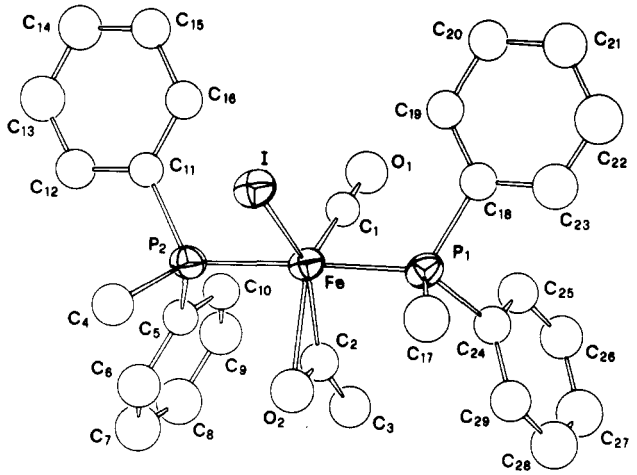

Figure 3. Molecular structure of complex **3d**.

(4) Description of the Molecular Structure of $[Fe(CO)(PMePh_2)_2(\eta^2\text{-}COCH_3)I]\cdot 2CH_2Cl_2$ (3d). Figure 3 shows a view of the molecular structure of **3d**. CH_2Cl_2 is removed from the picture. The overall symmetry is trigonal bipyramidal with the two phosphine ligands occupying the two trans positions (P(2)–Fe–P(1) = 178°). The methyl groups of the phosphine ligands are eclipsed, pointing between the iodine and the η^2-acyl groups. The ligands I, CO, and $COCH_3$ lie in the plane of the trigonal bipyramid. The oxygen atom of the η^2-acyl ligand lie in the cis position with respect to the iodine ligand. The Fe–O(2) bond length (2.250 Å) is strongly shorter than the same bond length in the η^1-acyl $COCH_3$ bond,[36] indicating the formation of the iron–oxygen bond. It is shorter than that in the ruthenium d^6 complex described by Roper et al.,[8b] in agreement with the larger atomic radius of ruthenium with respect to iron. The Fe–C(2) bond length (1.827 (11) Å) is shorter than that observed in the iron–alkyl complexes[37,38] (2.1 Å), indicating a strengthening of this bond owing the delocalization of the electronic density around the η^2-acyl structure. The C(2)-O(2) bond length (1.233 (14) Å) is longer than the C=O double bond (1.2 Å), indicating coordination of the oxygen atom to the iron atom and a back-donation of the d electrons into the antibonding orbital of the acyl group. The O(2)–Fe–C(2) angle (33.2 (4)°) is near to that observed in the other η^2-acyl structures.[8]

Discussion

All the structures of the complexes described are drawn in Figure 1. The structures of $[Fe(CO)_2L_2X_2]$, $[Fe(CO)_2L_2(MeCN)]$, and $[Fe(CO)_2L_2(R)X]$ are assigned on the basis of the IR and the ^1H NMR spectroscopic results (see text and table IV). The structure of the η^2-acyl complexes $[Fe(CO)L_2(\eta^2\text{-}COR)I]$ is assigned on the basis of the IR and ^1H NMR spectra and on the basis of an X-ray single-crystal structural determination of complex **3d**. The structure of the cluster $[Fe(CO)_2L_2]_3$ is questionable, since the spectroscopic evidence is not sufficient to assign this structure and an X-ray single-crystal determination has not up to now been possible.

The preparative method, described in this paper, owing to its general application, allows us to synthesize a large

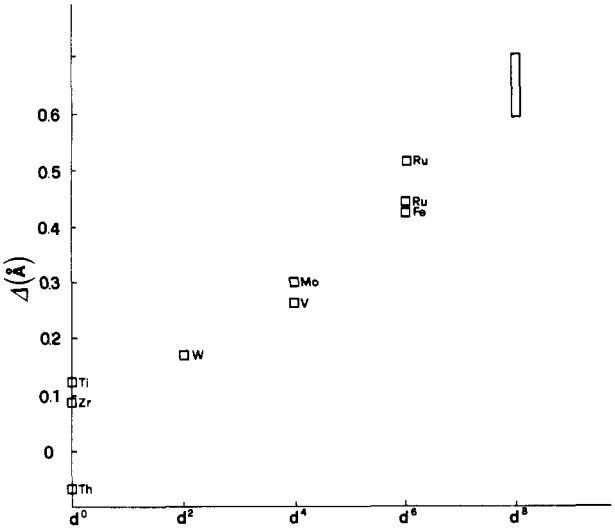

Figure 4. Δ values (see text) vs the formal d electron configuration of the complexes described in the literature[8] and of complex **3d**.

number of alkyl complexes with ligands of different steric hindrance[21] and basicity,[39] in order to discuss the electronic and steric features that stabilize the alkyl or the η^2-acyl structures. Up to now the η^2-acyl structures described in the literature[8] differ in the metal atom and in the ligands: no rationalization of these features has therefore been possible. Study of the factors that stabilize the η^2-acyl structures is an important tool for finding out the role of these structures in the mechanism of insertion of carbon monoxide in the metal–alkyl bond.[1a] The role of this structure in the activation complex, during the insertion reaction, has been recently studied theoretically[40,41] and has been excluded in the complexes of Pd and Pt. Another recent study on the insertion of carbon monoxide in complexes of Mn:$[RMn(CO)_4XY]$[42] enhanced the role of this structure in the stabilization of the unsaturated 16-electron intermediate, contrary to what was obtained by Hoffmann et al.;[43] only in complexes of group 4 metals and in the actinides did Hoffmann et al.[44] calculate stabilization of the η^2-acyl structures.

After these contrasting theoretical results, all experimental information ought to be of use for distinguishing between the various possibilities. As shown in Table IV, which reports the cone angle of the phosphine ligands, with L = PMe_3, PMe_2Ph, or $P(n\text{-}Bu)_3$, having a cone angle lower than 136°, the alkyl complexes $[Fe(CO)_2L_2(R)X]$ are stable. With L = $PMePh_2$, $PEtPh_2$, $P(i\text{-}Bu)_3$, or PPh_3, having a cone angle between 136° and 145°, the η^2-acyl structures $[Fe(CO)L_2(\eta^2\text{-}COR)I]$ are stabilized. With L = $P(i\text{-}Pr)_3$, having a cone angle of 160°, decomposition of complexes **6a** and **6b**, during the formation reaction, has been observed. These results suggest the steric hindrance is the most important factor in the stabilization of the η^2-acyl structure. In spite of the different basicity between $P(i\text{-}Bu)_3$ (ΔHNP[39] = 167) and PPh_3 ($\Delta(HNP)$[39] = 573) both these ligands stabilize the η^2-acyl structure. On the other hand PMe_3 and $P(i\text{-}Bu)_3$, having similar basicity but different steric hindrance, stabilize the alkyl structure and

(36) Bennett, M. A.; Kin-Chee Ho; Jeffery, J. C.; McLaughlin, G. M.; Robertson, G. B. *Aust. J. Chem.* **1982**, *35*, 1311–1321.
(37) Jablonski, C. R.; Wang, Y. P.; Taylor, N. J. *Inorg. Chim. Acta* **1985**, *96*, L17–L19.
(38) Chou, C. K.; Miles, D. L.; Bau, R.; Flood, T. C. *J. Am. Chem. Soc.* **1978**, *100*, 7271–7278.
(39) Streuli, C. A. *Anal. Chem.* **1959**, *31*, 1652–1654; **1960**, 985–987.
(40) Koga, N.; Morokuma, K. *J. Am. Chem. Soc.* **1985**, *107*, 7230–7231.
(41) Sakaki, S.; Kitaura, K.; Morokuma, K.; Ohkubo, K. *J. Am. Chem. Soc.* **1983**, *105*, 2280–2286.
(42) Ziegler, T.; Versluis, L.; Tschinke, V. *J. Am. Chem. Soc.* **1986**, *108*, 612–617.
(43) Berke, H.; Hoffmann, R. *J. Am. Chem. Soc.* **1978**, *100*, 7224–7236.
(44) Hoffmann, P.; Stauffert, P.; Tatsumi, K.; Nakamura, A.; Hoffmann, R. *Organometallics* **1985**, *4*, 404–406.

the η^2-acyl structure, respectively. When the cone angle of the ligands is more than 135°, the alkyl group cannot occupy a coordination position around the metal, stabilizing the η^2-acyl structure. The coordination of the lone pair of the oxygen of the acyl group to the metal saturates the electronic shell of the metal.

The CO and COR stretching bands and the chemical shifts of the $COCH_3$ group (Table IV) are very near in the various η^2-acyl structures. This is in agreement with a negligible effect of the electronic properties of the ligands in the stabilization of the η^2 structures and supports the conclusion that the stability of this bond is prevalently due to the nature and the oxidation state of the metal.

In order to support this conclusion we show in Figure 4 the Δ parameter as a function of the formal configuration of the d orbital of the η^2-acyl structures, characterized by X-ray determination. The Δ parameter is the difference between the metal–oxygen and the metal–carbon bond lengths of the η^2-acyl structure; it is reasonable to connect the stability of the η^2-acyl structure to this parameter.[8b] The lower is this value the more stable is the η^2 structure. Figure 4 shows a clear trend: as the number of d electrons increases, the stability of the η^2 structure decreases, whatever the nature of the ligands of the metal. Following the observed trend, we should obtain for the metals of the Pt(II) group a Δ value corresponding to the η^1-acyl structure, in agreement with the fact that with these d^8 metals no η^2 structure has ever been observed.

The small effect of the properties of the phosphine ligands on the stabilization of the η^2-acyl structures suggests these structures are intermediates in the insertion reaction of carbon monoxide in the alkyl complexes of iron(II). This conclusion is strengthened by a recent theoretical study on the d^6 Mn complexes,[42] which, in contrast with the previous conclusion of Hoffmann,[43] obtains a strong stabilization of the pentacoordinated intermediate via formation of the η^2-acyl structures.

Conclusion

The synthesis and the characterization of a long series of alkyl and η^2-acyl complexes of iron(II) have allowed us to obtain some conclusive results about the stability of the η^2-acyl structures. The η^2-acyl structures are predominantly stabilized by the steric hindrance of the other ligands. This stabilization is due to the impossibility for the alkyl group to coordinate around the metal.

On the basis of our results and those in the literature,[8] the stability of the η^2-acyl structure is due to the number of the d electrons on the metal. When this number is increased, the repulsion of the lone pair of the acyl oxygen increases and the η^2 structure is destabilized, whatever the nature of the other ligands (Figure 4).

The observation of the η^2-acyl structures in the iron(II) complexes suggests that these structures are present as intermediates in the insertion of carbon monoxide in the alkyl complexes of iron(II).

Acknowledgment. This work was supported by grants from the Consiglio Nazionale delle Ricerche (CNR, Rome) and the Ministero della Pubblica Istruzione (MPI, Rome).

Registry No. **1**, 62075-75-6; **1a**, 108188-38-1; **1b**, 108188-32-5; **1c**, 33542-07-3; **1c′**, 108188-44-9; **1c″**, 110433-10-8; **2**, 110455-78-2; **2a**, 108188-39-2; **2b**, 108188-33-6; **2c**, 108188-45-0; **3**, 51684-15-2; **3a**, 108188-40-5; **3b**, 108188-34-7; **3d**, 108188-47-2; **4**, 110455-79-3; **4a**, 108188-42-7; **4b**, 108188-36-9; **4c**, 108188-46-1; **5**, 110455-80-6; **5a**, 108188-43-8; **5b**, 108188-37-0; **5d**, 108188-49-4; **5d′**, 108188-50-7; **6**, 110418-11-6; **6a**, 110418-17-2; **7**, 110418-12-7; **8**, 51684-12-9; **8a**, 108188-41-6; **8b**, 108188-35-8; **8d**, 108188-48-3; **9**, 84622-99-1; **9a**, 110418-21-8; **9b**, 110418-18-3; **9d**, 110418-19-4; **10**, 110507-75-0; $[Fe(CO)_3(PMe_3)_2]$, 30230-16-1; $[Fe(CO)_3(PMe_3)_2Br]Br$, 62048-86-6; $[Fe(CO)_4Br_2]$, 18475-84-8; $[Fe(CO)_3(PMe_2Ph)Br_2]$, 110418-13-8; $[Fe(CO)_3(P(n\text{-}Bu)_3)Br_2]$, 110418-14-9; $[Fe(CO)_3P(i\text{-}Pr)_3)Br_2]$, 110418-15-0; $[Fe(CO)_3(P(i\text{-}Pr)_3)_2]$, 25921-45-3; $[Fe(CO)_4Cl_2]$, 21475-90-1; $[Fe(CO)_3(PEtPh_2)Br_2]$, 110418-16-1; $[Fe(CO)_3(PPh_3)Br_2]$, 110455-81-7; $[Fe(CO)_3(PPh_3)_2]$, 21255-52-7; $[Fe(CO)_2(PPh_3)_2(Et_2O)]$, 110418-20-7.

Supplementary Material Available: Tables 1S–3S, calculated hydrogen positions and complete listings of bond lengths and angles for complex **3d** (5 pages); Table 4S, observed and calculated structure factors for complex **3d** (15 pages). Ordering information is given on any current masthead page.